Polyanion-Induced α-Helical Structure of a Synthetic 23-Residue Peptide Representing the Lysine-Rich Segment of the N-Terminal Extension of Yeast Cytoplasmic Aspartyl-tRNA Synthetase†

Fabrice Agou,‡ Yinshan Yang,§ Jean-Claude Gesquière,|| Jean-Pierre Waller,‡ and Eric Guittet*,§

Laboratoire d'Enzymologie, Centre National de la Recherche Scientifique, 91198 Gif-sur-Yvette Cedex, France, Laboratoire de Résonance Magnétique Nucléaire, Institut de Chimie des Substances Naturelles, Centre National de la Recherche Scientifique, 91198 Gif-sur-Yvette Cedex, France, and Institut Pasteur de Lille, Service de Chimie des Biomolécules, URA 1309 du Centre National de la Recherche Scientifique, B. P. 245, 59019 Lille Cedex, France

Received July 14, 1994; Revised Manuscript Received October 28, 1994®

ABSTRACT: Conformational studies were performed on the synthetic tricosapeptide *N*-acetyl-SKKALKKLQKEQEKQRKKEERAL-amide, representing the highly basic segment (residues 30−52) of the N-terminal extension of yeast cytoplasmic aspartyl-tRNA synthetase. Circular dichroism experiments show that, in aqueous solution at neutral pH, the peptide adopts a random conformation. The effects of pH, temperature, addition of trifluoroethanol (TFE), and titration with polyanions on the conformation of the peptide were studied. In TFE or in the presence of an equimolar concentration of $(phosphate)_{18}$, the peptide adopts a 100% α-helical conformation. A partially α-helical conformation is induced by $(phosphate)_4$ or $d(pT)_8$ (respectively 40% and 35% helical content). Raising the pH in aqueous solution promotes 75% α-helicity, with a transition p*K* of 9.9 reflecting deprotonation of lysine residues. On the basis of these results, nuclear magnetic resonance studies were carried out in TFE as well as in aqueous solution in the presence of $(phosphate)_{18}$, to determine the structure of the molecule. Complete ^1H resonance assignments were obtained by conventional two-dimensional NMR techniques. A total of 138 inter-proton constraints derived from NOESY experiments were used to calculate the three-dimensional structure by a two-stage distance geometry/simulated annealing procedure. The two deduced structures were highly similar and show that nine cationic residues are segregated on one face of a helical structure, providing an ideal polycationic interface for binding to polyanionic surfaces.

Compared to its prokaryotic homologue, yeast cytoplasmic aspartyl-tRNA synthetase carries a cationic N-terminal extension of about 100 amino acid residues (Sellami *et al.*, 1986; Eriani *et al.*, 1990). Similar positively charged N-terminal extensions of varying length and sequence were found in other yeast aminoacyl-tRNA synthetases, including valyl-, threonyl-, and lysyl-tRNA synthetases [reviewed in Mirande (1991)]. It was shown previously that lower eukaryotic aminoacyl-tRNA synthetases generally display much higher affinity for polyanionic chromatographic supports than do the corresponding enzymes from prokaryotes (Cirakoglu & Waller, 1985). The finding that excision of the lysine-rich N-terminal extensions from yeast lysyl- (Cirakoglu & Waller, 1985) and aspartyl-tRNA synthetases (Lorber *et al.*, 1988; Eriani *et al.*, 1991) generates modified enzymes that retain catalytic activity yet display much reduced affinity for immobilized heparin supported the view that the high affinity toward polyanionic carriers was mainly conferred by their cationic N-terminal extensions. In line with this conclusion, it was recently shown that whereas yeast valyl- and lysyl-tRNA synthetases bind strongly to microtubules *in vitro*, via electrostatic interactions with the exposed C-terminal polyanionic tails of α- and β-tubulins, deletion of the N-terminal cationic extension of lysyl-tRNA synthetase abolishes this association (Melki *et al.*, 1991).

The cationic (mainly lysine) residues contained within the N-terminal extensions of the aforementioned enzymes are mostly confined to a limited segment of these extensions which, according to structure predictions, has a high propensity to fold into an α-helical structure. In the case of aspartyl-tRNA synthetase, this putative helical segment spans residues 30−52 and contains eight lysine, two arginine, and four glutamic acid residues. Morever, in each of the four cases, a helical wheel projection of the relevant sequences shows anisotropic distribution of the basic residues, which segregate to one face of the helix (Lorber *et al.*, 1988; Mirande & Waller, 1988). Such putative helices are attractive candidates for binding to polyanionic surfaces. We previously suggested that the evolutionary acquisition of polycationic structural modules by lower eukaryotic aminoacyl-tRNA synthetases may ensure their spatial confinement at the site of protein synthesis, through dynamic electrostatic interactions with polyanionic components of the translation apparatus (Cirakoglu & Waller, 1985; Mirande, 1991).

Further understanding of the role of these cationic structural modules will require the elucidation of their three-dimensional structure. To date, the only lower eukaryotic aminoacyl-tRNA synthetase whose structure was determined by X-ray crystallography is yeast aspartyl-tRNA synthetase.

† Supported by grants from the Centre National de la Recherche Scientifique, from the Ligue Nationale contre le Cancer, and from the Association pour la Recherche contre le Cancer.

* To whom correspondance should be addressed.
‡ Laboratoire d'Enzymologie.
§ Laboratoire de Résonance Magnétique.
|| Institut Pasteur de Lille.

® Abstract published in *Advance ACS Abstracts,* December 1, 1994.

0006-2960/95/0434-569$09.00/0

The structure of the enzyme complexed with its cognate tRNA was recently solved to 0.29-nm resolution (Cavarelli *et al.*, 1993). However, the first 65 residues from the N-terminus could not be traced in the electron density map and are presumably disordered. It is also noteworthy that, in the absence of tRNA, N-terminally truncated forms of the enzyme lacking the charged segment could be readily crystallized (Lorber *et al.*, 1987), whereas the native enzyme has failed to crystallize so far. Because of the present limitations of the crystallographic approach in the determination of the conformation of the cationic N-terminal extremity of yeast aspartyl-tRNA synthetase, we have synthesized the polypeptide representing residues 30−52 of its sequence and have examined the solution structure of this polypeptide under various conditions, using circular dichroism and nuclear magnetic resonance spectroscopy.

EXPERIMENTAL PROCEDURES

Materials. Sodium octadecaphosphate ($P_{18\pm3}$), sodium tetraphosphate (P_4), and the oligodeoxynucleotides $d(pT)_8$ and $d(pA)_8$ were from Sigma.

Peptide Synthesis and Purification. The tricosapeptide Ac-SKKALKKLQKEQEKQRKKEERAL-NH_2 was synthesized by the solid-phase method (Merrifield, 1963) in an Applied Biosystems 430 A peptide synthesizer (Foster City, CA), using optimized procedures for NMP cycles. The side chains of BOC-amino acids were protected as follows: tosyl (Arg), cyclohexyl (Glu), 2-chlorobenzyloxycarbonyl (Lys), and Bzl (Ser). The first residue was coupled to a MBHA resin, in order to yield a C-terminal amidated peptide. All coupling was performed only once with HOBt esters, and a capping step with acetic anhydride took place at the end of each cycle. Introduction of the last residue was followed by the removal of the BOC group and an acetylation of the N^{α} group of the serine. The peptide was cleaved from the resin using anhydrous HF in the presence of 10% *p*-cresol at −5 °C for 60 min. After HF removal, the peptide was washed with cold ethyl ether, extracted with 5% acetic acid, and then submitted to lyophilization.

The crude peptide was purified by gel filtration (Fractogel TSK HW-40 S) and then by semipreparative HPLC on a Nucleosil 100-5 C_{18} column, 0.8 × 50 cm, using a linear gradient of 4−28% acetonitrile in 0.05% TFA (flow rate, 2 mL/min; linear gradient, 0.4%/min). The pure peptide was characterized by amino acid analysis on a Beckman 6300 amino acid analyzer (Beckman Instruments, Fullerton, CA) and by mass spectrometry using a PDMS time of flight BioIOn-20 spectrometer (Applied Biosystems Inc.), which gave a clean positive spectrum with $[M+H]^+$ at m/z = 2968.7. The peptide concentration of a neutralized stock solution was determined by quantitative amino acid analysis performed in triplicate. Aliquots of the stock solution were stored at −80 °C.

CD[1] *Spectroscopy.* Circular dichroism spectra were recorded digitally from 190 to 260 nm for experiments with peptide alone and to 350 nm for those in the presence of oligonucleotides, using a JOBIN YVON Mark V spectropolarimeter equipped with a data processor and a temperature-controlled cell holder. The spectrometer was calibrated with (+)-10-camphorsulfonic acid. Cells with different path lengths (from 1 to 5 mm) were used, depending on the concentration of peptide and oligonucleotides. Spectra were recorded with a scanning window (i.e., the product of the time constant and the rate of scanning) kept below 0.33 nm (Hennesey & Johnson, 1982), using a bandwidth of 1 nm. Each spectrum is the result of the average of three scans taken from the same sample minus the average of three scans from a reference sample containing an identical solution without the peptide. The secondary structure of the peptide was determined by fitting the CD spectra to poly(lysine) reference spectra (Yang *et al.*, 1986), by a least squares fitting procedure using the MDFITT program developed by M. Desmadril (Laboratoire d'Enzymologie Physicochimique et Moléculaire, Faculté des Sciences, 91405 Orsay, France).

NMR Spectroscopy. The samples analyzed by NMR contained 2 mM peptide in 0.5 mL of TFE (CF3CD2OH) and 2 mM peptide in the presence of 4 mM octadecaphosphate or 9 mM tetraphosphate, both in 0.5 mL of aqueous solution adjusted to pH 4.5. ^1H NMR experiments were recorded on a Bruker AM-600 spectrometer equipped with an Aspect-3000 computer. All two-dimensional spectra were recorded in the pure-phase sensible mode by application of TPPI (Redfield & Kuntz, 1975; Marion & Wüthrich, 1983). The large solvent resonance was suppressed by presaturation during the relaxation delay. For the NOESY(Jeener *et al.*, 1979; Kumar *et al.*, 1980) experiment, presaturation was also applied during the mixing time. Spectra were acquired with 2048 data points in t_2 and 512 points in t_1 with a spectral width of 6493.5Hz, in the temperature range of 15−25 °C. The chemical shift values of protons were calibrated by using the resonance position of the solvent line relative to tetramethylsilane (CH of CF_3CHDOH, with a chemical shift of 3.98 ppm, or H_2O of the residual water, with a chemical shift of 4.878 ppm, at 15 °C).

The 2D TOCSY experiment (Braunschweiler & Ernst, 1983; Davis & Bax, 1985) was performed with a MLEV-17 mixing sequence (Davis & Bax, 1985), with a mixing time of 70 ms. The 2D NOE spectra were recorded with a 32-step phase cycle (States *et al.*, 1982) with mixing times of 100, 150, and 300 ms.

TOCSY and NOESY data were processed on a IBM Risc 6000 computer using the software GIFA, which was developed in our laboratory (M.-A. Delsuc, M. Robin and V. Stoven, unpublished). The data were apodized by a shifted cosine function in both dimensions. Zero filling was used to obtain a spectral data matrix of 1K × 4K real points. The final spectra were corrected for a distorted baseline in *F*1 and *F*2. Peak integrals were determined by the PARIS subprogram (Stoven *et al.*, 1989) from the NOESY spectra with a mixing time of 100 ms.

Structure Calculations. The volumes of the integrated NOESY cross peaks were calibrated against the known distance (0.173 nm) of the geminal protons of the side-chain amide of Q15. Structures were calculated by using a two-stage distance geometry/simulated annealing procedure (Nilges *et al.*, 1988). The metric matrix distance geometry part of the calculations was carried out using the VEMBED program, with 1000 steps of optimization after embedding.

The annealing protocol used was essentially that described by Nilges *et al.* (1988). Simulated annealing was carried

[1] Abbreviations: TFE, trifluoroethanol; CD, circular dichroism; 2D NMR, two-dimensional nuclear magnetic resonance; NOE, nuclear Overhauser effect; NOESY, nuclear Overhauser effect spectroscopy; TOCSY, total correlation spectroscopy; TPPI, time proportional phase increment.

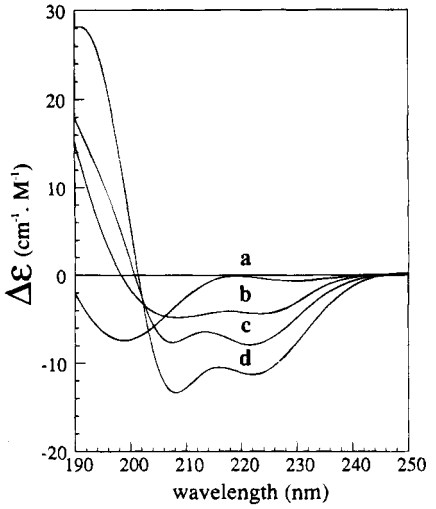

FIGURE 1: CD spectra of the tricosapeptide under various conditions: 10 μM, in aqueous solution at pH 7.0 and 22 °C (curve a), at pH 11 and 22 °C (curve b) or 1 °C (curve c), or in TFE (curve d).

out with the program XPLOR (Brünger, 1990). The NOE distance restraints are represented by square-well potentials with variable force constants. The annealing protocol consists in setting the initial weight on the repulsive van der Waals term to a very low value to allow atoms to pass through each other easily. The structural folding is then determined mainly by the experimental restraints rather than by high van der Waals interactions. The procedure consists in five phases: (i) One thousand cycles of Powell minimization in order to retrieve bad nonbonded contacts in the VEMBED structures defines the first phase. This is followed by (ii) 15-ps dynamics with a time step of 2 fs at 1000 K and (iii) 10-ps dynamics at 1000 K. During the last period, the force constant k_{repel} is increased from 0.002 to 0.1 by multiplying it by a factor of 1.5 every picosecond. (iv) The temperature is then cooled to 300 K by 25 K steps of 0.1 ps while all the force constants are kept at their final values, and (v) the protocol is concluded by 1500 cycles of Powell minimization. Initial model building of the structures by distance geometry was carried out on an Alliant VFX40. This procedure took 15 min per structure. The dynamical simulated annealing protocol was performed on a IBM 3090-VF computer. The corresponding procedure takes about 1 h for each structure. The resulting computed structures were displayed and inspected on a Silicon Graphics Personal Iris 4D25, using the Insight II program from Biosym Technologies.

RESULTS

Circular Dichroism. Spectra of the tricosapeptide recorded under various conditions are shown in Figure 1. In the presence of the helix-stabilizing solvent TFE at ≥80% (v/v), at 22 or 1 °C, the spectrum was characteristic for an α-helix (curve d). The $\Delta\epsilon$ value of -11.1 cm^{-1} M^{-1}, which was independent of the peptide concentration in the range 4−50 μM, corresponds closely to the value reported for the fully helical conformation of poly(lysine) in water at pH 11.1 and 22 °C (Yang *et al.*, 1986). In aqueous solution, the conformation of the peptide was strongly pH-dependent. At pH 7.0, both at 22 and 1 °C, the spectrum was characteristic for a random coil (curve a). The profile was independent

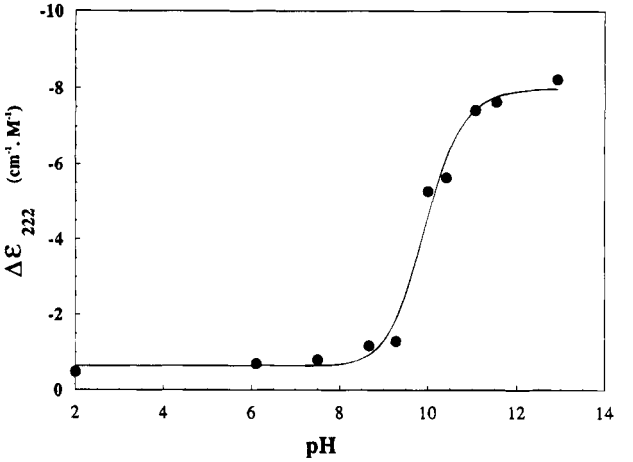

FIGURE 2: pH dependence of the differential molar CD extinction coefficient ($\Delta\epsilon$) at 222 nm of the tricosapeptide (5 μM). Spectra were recorded in aqueous solution at 1 °C.

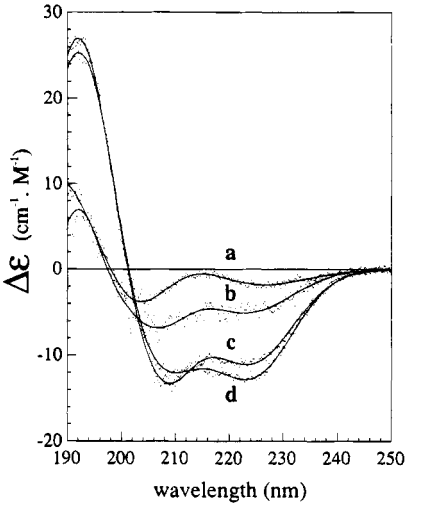

FIGURE 3: CD spectra of the tricosapeptide (4.5 μM) in the presence of 10 mM sodium phosphate (monophosphate) at pH 7.0 (curve a) and in the same buffer containing a 15 M excess of tetraphosphate (P_4) (curve b) or a 3 M excess of octadecaphosphate (P_{18}) (curve d). The signal of the peptide in TFE (curve c) is shown for reference. All spectra were recorded at 12 °C.

of concentration in the range of 2−150 μM peptide. At pH 11.0 and 22 °C, the CD spectrum of the peptide was indicative of a high fractional content of helical residues (curve b), which markedly increased on lowering the temperature to 1 °C (curve c). The dependence of $\Delta\epsilon_{222}$ on pH at 1 °C is shown in Figure 2. The observed changes correspond to a coil to helix transition having a midpoint at pH 9.9, reflecting deprotonation of the lysine residues. The plateau value of $\Delta\epsilon_{222}$, -8.3 cm^{-1} M^{-1} at alkaline pH, corresponds to a helix content of about 75%, relative to the $\Delta\epsilon_{222}$ value of -11.1 cm^{-1} M^{-1} in TFE taken as 100%.

Structural Transition Induced by Polyanions. To examine the effect of polyanions on the conformation of the tricosapeptide, CD spectra were recorded in the presence of various polyanionic molecules. Figure 3 shows the spectra obtained in 10 mM sodium phosphate, pH 7.0, and in the same buffer containing a 15 M excess of tetraphosphate or a 3 M excess of octadecaphosphate. The α-helical contents were estimated to be 5%, 40%, and 100%, respectively, relative to the reference spectra of the peptide in TFE (100% α-helical) and in aqueous solution at neutral pH (random coil). For

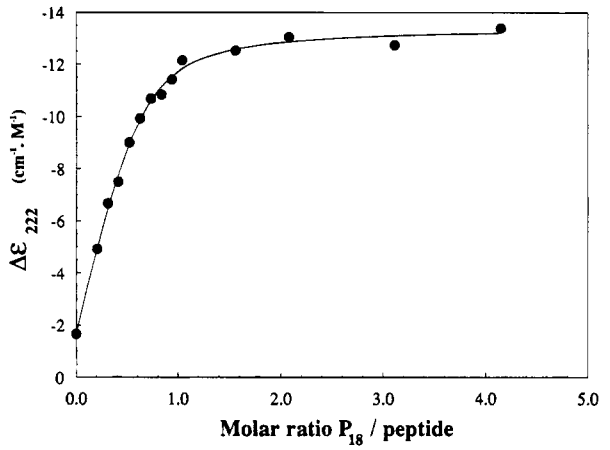

FIGURE 4: Titration by octadecaphosphate (P_{18}) of the tricosapeptide (4.5 μM) in 10 mM sodium phosphate buffer, pH 7.0, at 12 °C.

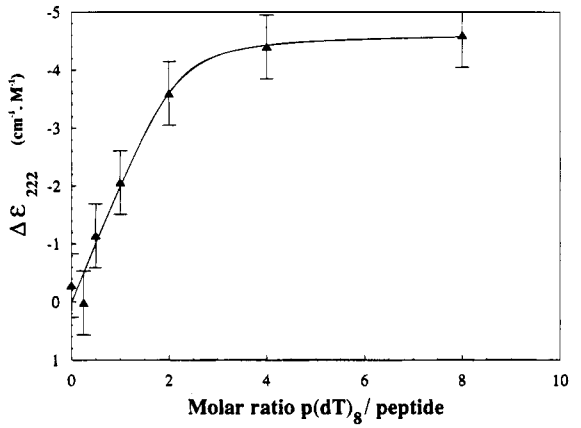

FIGURE 5: Titration by $(dT)_8$ of the tricosapeptide (2 μM) in 20 mM Tris-HCl, pH 7.2, at 20 °C. The spectra were corrected for the contribution of $(dT)_8$ alone.

the two oligophosphates, spectra recorded in 10 mM sodium acetate at pH 4.5, the pH conditions in the NMR experiments, were identical to those obtained in 10 mM sodium phosphate, pH 7.0, at the same temperature (12 °C). It should be noted that while the CD spectra of the peptide in TFE or in the presence of octadecaphosphate show identical α-helical contents, they display slightly different ellipticity values for the positive band at 192 nm and for the two negative bands at 208 and 222 nm. While poorly understood, these differences were found to be highly reproducible.

Titration of the peptide by octadecaphosphate (Figure 4) shows that the amount required to induce a fully α-helical structure extrapolates to an [octadecaphosphate]:[peptide] molar ratio of 0.85. Given the uncertainty concerning the length of the poly(phosphate) (18 ± 3), the result is compatible with a 1:1 stoichiometric association.

The effect of oligodeoxynucleotides on the structure of the tricosapeptide was also examined. In the presence of $d(pT)_8$, the CD spectrum of the peptide, after subtraction of the spectrum of the oligonucleotide alone, displayed minima at 208 and 222 nm characteristic for an α-helix. A plot of the oligonucleotide concentration dependence of $\Delta\epsilon_{222}$ upon titration of 2 μM peptide with $d(pT)_8$ in water at pH 7.0 and 20 °C is shown in Figure 5. The $\Delta\epsilon$ plateau value of −4.6 cm^{-1} M^{-1} attained in the presence of a 4-fold molar excess of $d(pT)_8$ corresponds to a helical content of about 35%. At 1 °C, the same plateau value of $\Delta\epsilon$ was reached with an equimolar amount of $d(pT)_8$. Identical results were obtained when $d(pA)_8$ was substituted for $d(pT)_8$ (results not shown). The absence of sequence specificity supports the conclusion that ionic interactions between the cationic groups of the peptide and the phosphate groups of the oligodeoxyribonucleotide are responsible for the structural transition induced.

Nuclear Magnetic Resonance. On the basis of the CD data and considering the problem of the rapid amide proton exchange with water at basic pH, all NMR experiments were carried out first in 100% TFE solution at 25 °C. Under these conditions the peptide is completely converted to an ordered helical structure. Sequence-specific assignments were obtained by means of two-dimensional NMR spectroscopy as described (Wüthrich *et al.*, 1982, 1983; Billeter *et al.*, 1982; Strop *et al.*, 1983; Zuiderweg *et al.*, 1983). In short, this involves first identification of the spin systems using TOCSY experiments, followed by NOESY experiments to identify through-space short (<0.5 nm) inter-proton contacts, of which the interresidue NH_i-NH_{i+1}(d2) and αH_i-NH_{i+1}(d1) connectivities are the most important for the purposes of sequential assignments. Figure 6A presents an expansion of the NOESY spectrum and shows consecutive strings of dNN NOEs in the amide region of the phase-sensitive NOESY spectrum showing the assignment from residues 1−23. A summary of the assignments of the proton resonances is given in Table 1. It should be noted that, without exception, there is only one resonance position per proton. Thus we can conclude that the peptide adopts either one conformation or more than one, each in fast exchange on the chemical-shift time scale with the others. As discussed in detail by Wüthrich *et al.* (1984), the secondary structure can be deduced by a qualitative inspection of the NOESY spectrum. From the NOESY spectra of the peptide, strong αH_i-NH_i (intraresidue) and NH_i-NH_{i+1}(d2) connectivities and weak αH_i-NH_{i+1}(d1) connectivities are seen for all the interresidue steps. The βH_i-NH_{i+1} and αH_i-NH_{i+3} connectivities are also observed for all interresidue steps with the exception of those appearing in the overlapped regions. These observations are indicative of an helical structure and agree well with the CD results above.

Evaluation of the Distance Constraints. Throughout this work, the distances were measured from the individual cross-relaxation rates (a_{ij}) (NOE buildup rate) and comparison to that (a_{ref}) for protons with a known fixed distance, according to the equation $r_{ij}/r_{ref} = (a_{ref}/a_{ij})/6$. The use of such scaling to a reference distance is only valid if the unknown proton pair has the same correlation time as the reference proton pair. Thus the choice of the reference fixed distance is important if the molecule under study exhibits internal motion in addition to the global motion in solution. In the case of the 23-residue peptide in TFE, the terminal NH_2 of Q15 was selected as the reference peak pair with a distance of 0.173 nm. In the spectra with a mixing time of 100 ms, peak intensities were determined by integration. The NOE buildup was assumed to be linear for this short mixing time (Kline *et al.*, 1988), and thus proton distances were calculated by using the $1/r^6$ dependence for the nuclear Overhauser effect in rigid molecules. All the NH_i-NH_{i+1} values fall in a distance range of 0.27−0.28 nm; the αH_i-NH_is, in a distance range of 0.26−0.27 nm; the αH_i-NH_{i+1}s, in a distance range of 0.33−0.35 nm; and the βH_i-NH_{i+1}s, 0.29−0.30 nm. For the peaks with weak intensities, which are difficult to integrate, only an approximate distance was obtained. Ac-

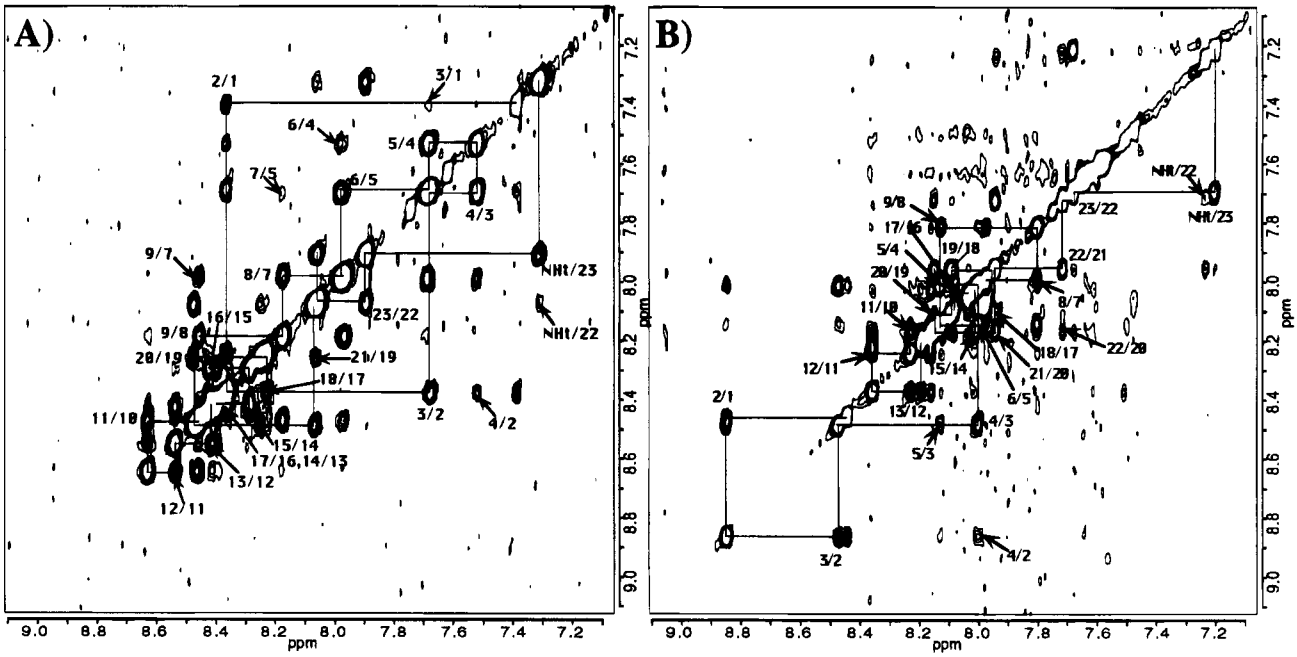

FIGURE 6: Expanded regions of the NOESY spectra of the tricosapeptide in TFE at 25 °C (A) and in aqueous solution in the presence of octadecaphosphate at 15 °C (B), illustrating all of the NH_i-NH_{i+1} and some of the NH_i-NH_{i+2} connectivities (mixing time, 300 ms).

cording to the approach of Wüthrich and his collaborators, who use the known sequential distances in the different secondary structures found in proteins, distances of 0.35 and 0.40 nm were used for the weak NOE contacts of αH_i-NH_{i+3} and NH_i-NH_{i+2}, respectively.

Structural Transition Induced by Polyanions. A folding into an α-helical structure similar to that obtained in TFE was observed upon addition of 2 mol equiv of octadecaphosphate in aqueous solution. This is shown in Figure 6B, where the spectrum of the NH−NH region is compared to that obtained in TFE. The chemical shifts of the tricosapeptide in the presence of the octadecaphosphate are listed in Table 1. A significant upfield shift is experienced by almost all Hα protons, as compared to the chemical shifts of a random-coiled peptide. Such a situation is often related to an α-helix folding (Wishard *et al.*, 1992). NMR spectra taken in the presence of 4.5 mol equiv of tetraphosphate demonstrated a similar trend even though the proton connectivities disclosed were of poorer quality, especially for the long-range connectivities (results not shown). This probably reflects an equilibrium between the unfolded and folded forms, as suggested by the CD experiments. Almost identical sets of distances could be measured from the spectra obtained either in 100% TFE or upon interaction with octadecaphosphate in aqueous solution. The three-dimensional reconstruction was performed from the set of distances obtained in 100% TFE, but the results would clearly be similar in the case of the interaction with the oligophosphate.

Structure Computation and Analysis. After quantitation of the NOE data, a total of 138 inter-proton distance restraints, derived from the NOESY spectrum with a mixing time of 100 ms, were used to calculate three-dimensional structures. This distance set is somewhat limited, due to the numerous chemical shift degeneracies, and is insufficient to refine the entire molecule. The calculations were thus principally aimed at defining the helical motif. The structures were calculated on the basis of the NMR data by using a combination of distance geometry (Crippen, 1977; Havel *et al.*, 1983; Kuntz *et al.*, 1979) and dynamical simulated annealing methods (Brünger *et al.*, 1986). The metric matrix distance geometry part of the calculations was carried out using the VEMBED program, a vectorized version of the EMBED program (written by G. M. Crippen, I. D. Kuntz, and T. Havel). The dynamic simulated annealing calculations were performed using the X-PLOR program (Brünger, 1990).

Initially, 20 conformations were computed with VEMBED, with 1000 steps of optimization after embedding. The structures had no distance violations greater than 0.04 nm, but three of them gave left-handed helices (structures 1, 5, and 6). We therefore decided to carry out the dynamical simulated annealing protocol on the right-handed conformations only. Seventeen VEMBED structures of the peptide were chosen for this purpose using the X-PLOR program. Except for structure 20, which had five violations of the NOE constraints greater than 0.03 nm and had an E_{total} energy value as high as 135.0 kJ/mol, these other calculated structures showed no NOE constraint violations greater than 0.03 nm and had an average energy $E_{total} = 76.45 \pm 2.39$ kJ/mol. The analysis of the final structures clearly shows that eight of these structures are very similar (structures 3, 4, 9, 13, 14, 15, 16, and 19) as compared by the root mean square deviation values of the backbone atoms between each structure pair. The other eight structures (structures 2, 7, 8, 10, 11, 12, 17, and 18), while similar to each other, are slightly different from the first family. The superpositions of the backbone atoms of the structures of the two families are shown in Figure 7. Table 2 gives the root mean square deviations of the positions of the backbone atoms for all structure pairs in the two families. The difference is merely a more pronounced curvature of the α-helix in family 2, with the charged amino acid side chains located at the convex part of the molecule. NMR and molecular dynamic results demonstrate that, in the helical conformation of the peptide, the charged amino acid residues are asymmetrically distributed as shown in Figure 8. At neutral pH there are eight

Table 1: ^{1}H NMR Chemical Shifts of the Tricosapeptide at 25 °C in TFE and at 15 °C in H_2O in the Presence of Octadecaphosphate

residue[a]	NH	αH	βH	γH	δH	others
(Ac)						2.13 (Ac-CH_3)
						2.00 (Ac-CH_3)
Ser1	7.37	4.54	4.15, 3.96			
	9.22	4.29	4.07, 3.86			
Lys2	8.32	4.22	1.99, 1.91	1.91, 1.81	1.70, 1.58	3.10 (εCH)
	9.77	4.00	1.90, 1.79	1.35, 1.35	1.69, 1.53	2.93 (εCH)
Lys3	7.68	4.05	1.89, 1.76	1.64, 1.64	1.52, 1.52	3.10 (εCH)
	9.26	3.96	1.84, 1.70	1.37, 1.37	1.52, 1.52	2.94 (εCH)
Ala4	7.53	4.15	1.59			
	8.63	4.03	1.40			
Leu5	7.68	4.22	1.89, 1.89	1.76	0.94, 0.94	
	8.80	4.09	1.74, 1.63	1.56	0.84, 0.82	
Lys6	7.98	4.22	2.03, 2.03	1.84, 1.67	1.54, 1.54	3.15 (εCH)
	8.63	4.07	1.87, 1.87	1.40, 1.40	1.65, 1.53	2.89 (εCH)
Lys7	7.98	4.05	2.12, 2.03	1.80, 1.67	1.54, 1.54	3.10 (εCH)
	8.59	4.00	1.86, 1.86	1.39, 1.39	1.64, 1.54	2.91 (εCH)
Leu8	8.18	4.20	1.97, 1.97	1.87	0.99, 0.99	
	8.36	4.10	1.71, 1.71	1.59	0.89, 0.84	
Gln9	8.45	4.10	2.42, 2.42	2.72, 2.72		6.15, 6.78 (δNH)
	8.80	4.01	2.17, 2.07	2.48, 2.33		7.95, 7.12 (δNH)
Lys10	8.44	4.16	2.19, 2.19	2.01, 1.83	1.75, 1.67	3.00 (εCH)
	8.84	3.95	1.92, 1.86	1.37, 1.37	1.65, 1.54	2.92 (εCH)
Glu11	8.63	4.20	2.33, 2.71	2.44, 2.44		
	8.94	4.03	2.23, 2.11	2.50, 2.50		
Gln12	8.54	4.11	2.47, 2.24	2.76, 2.47		6.16, 6.83 (δNH)
	9.11	4.01	2.22, 2.02	2.56, 2.35		7.98, 7.10 (δNH)
Glu13	8.41	4.13	2.46, 2.29	2.77, 2.55		
	8.88	4.09	2.18, 2.09	2.47, 2.42		
Lys14	8.40	4.00	2.12, 2.00	2.46, 2.46	2.29, 2.29	3.09 (εCH)
	8.84	4.05	1.86, 1.86	1.37, 1.37	1.65, 1.54	2.92 (εCH)
Gln15	8.28	4.15	2.38, 2.28	2.60, 2.60		6.29, 7.05 (δNH)
	8.65	3.97	2.14, 2.03	2.42, 2.40		8.11, 7.16 (δNH)
Arg16	8.41	4.13	2.08, 2.08	1.91, 1.91	3.29, 3.37	6.85 (εNH)
	8.68	4.02	1.90, 1.70	1.54, 1.54	3.19, 3.15	7.94 (εNH)
Lys17	8.35	4.12	2.16, 1.94	1.76, 1.76	1.63, 1.63	3.10 (εCH)
	8.74	3.96	1.85, 1.85	1.32, 1.32	1.63, 1.56	2.90 (εCH)
Lys18	8.21	4.03	2.11, 2.04	1.80, 1.80	1.50, 1.50	3.06 (εCH)
	8.55	3.90	1.88, 1.88	1.36, 1.36	1.61, 1.54	2.90 (εCH)
Glu19	8.24	4.12	2.45, 2.26	2.83, 2.56		
	8.76	4.03	2.14, 2.04	2.49, 2.35		
Glu20	8.45	4.10	2.55, 2.29	2.85, 2.85		
	8.84	4.02	2.08, 2.08	2.49, 2.34		
Arg21	8.04	4.21	2.07, 2.07	1.84, 1.84	3.27, 3.39	6.87 (εNH)
	8.55	4.07	1.86, 1.77	1.64, 1.64	3.17, 3.11	7.60 (εNH)
Ala22	8.04	4.29	1.59			
	8.25	4.16	1.39	1.53		
Leu 23	7.87	4.42	1.91, 1.91	1.70	0.98, 0.98	
	8.20	4.13	1.72, 1.72		0.86, 0.81	
(NH_2)						6.15, 7.3
						7.56, 7.56

[a] The first entry for each residue is in TFE; the second is in aqueous solution in the presence of octadecaphosphate. Chemical shifts are relative to the CF_3CHDOH resonance set at 3.98 ppm relative to TMS or to the H_2O resonance set at 4.88 ppm relative to TMS.

positive charges on one face of the helix and a net charge of 2− on the opposite face. The helical structure results in a surface of high positive charge density ideally oriented for interaction with the phosphate groups of the poly(phosphate).

DISCUSSION

In the present study, circular dichroism spectra indicate that the tricosapeptide is unstructured in water but becomes fully helical in the presence of a molar equivalent of octadecaphosphate, similarly to the effect induced by TFE. Similar increases of α-helical content upon addition of inorganic poly(phosphate)s have been recently reported for a pentacosapeptide representing the RNA-binding N-terminus of cowpea chlorotic mottle virus coat protein (Van der Graaf

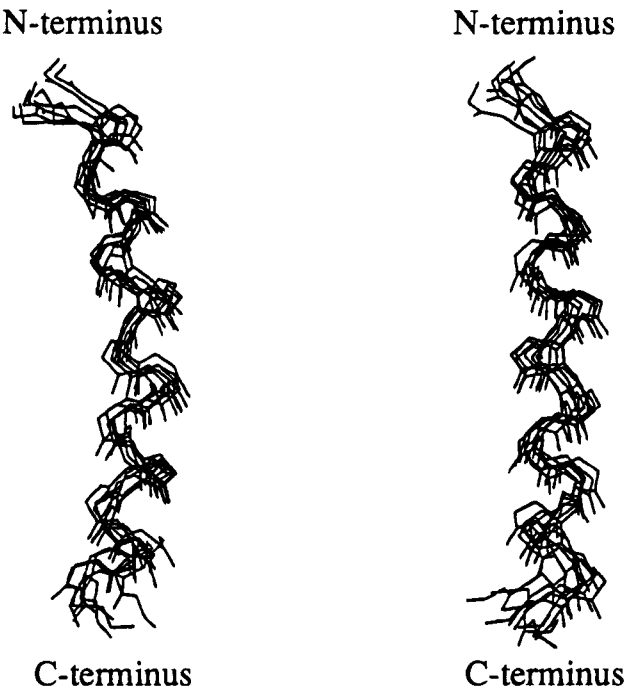

FIGURE 7: Backbone traces for the eight converged and energy-minimized conformations in family 1 (3, 4, 9, 13, 14, 15, 16, and 19) (left) and in family 2 (2, 7, 8, 10, 11, 12, 17, and 18) (right).

Table 2: Root Mean Square Deviation of the Backbone Atom Positions for the Structure Pairs of the Polypeptide[a]

(a) Family 1

	structure							
structure	3	4	9	13	14	15	16	19
3		0.133	0.136	0.149	0.150	0.108	0.101	0.121
4	0.133		0.200	0.220	0.129	0.162	0.132	0.143
9	0.136	0.200		0.158	0.160	0.064	0.123	0.105
13	0.149	0.220	0.158		0.127	0.138	0.220	0.196
14	0.150	0.129	0.160	0.127		0.137	0.175	0.143
15	0.108	0.162	0.064	0.138	0.137		0.110	0.101
16	0.101	0.132	0.123	0.220	0.175	0.110		0.072
19	0.121	0.143	0.105	0.196	0.143	0.101	0.072	

(b) Family 2

	structure							
structure	2	7	8	10	11	12	17	18
2		0.128	0.130	0.164	0.081	0.152	0.113	0.158
7	0.128		0.197	0.085	0.135	0.095	0.152	0.109
8	0.130	0.197		0.220	0.114	0.126	0.103	0.147
10	0.164	0.085	0.220		0.145	0.068	0.186	0.135
11	0.081	0.135	0.114	0.145		0.126	0.135	0.143
12	0.152	0.095	0.126	0.068	0.126		0.170	0.121
17	0.113	0.152	0.103	0.186	0.135	0.170		0.110
18	0.158	0.109	0.147	0.135	0.143	0.121	0.110	

[a] Root mean square deviations are given in nm.

et al., 1992). However, in that case, the increase in α-helicity was rather limited, since the conformation was already 20−21% α-helical at 10 °C in water in the absence of octadecaphosphate and rose to 42% in its presence. The structuralization was in fact limited to the region between residues 9 and 17. In our case, on the basis of the CD and NMR results, the α-helical conformation induced by octadecaphosphate extends throughout the sequence, whereas in the absence of inducer the solution structure is entirely random coil. Moreover, a molar equivalent of octadecaphosphate was sufficient to induce the α-helical conformation, pointing

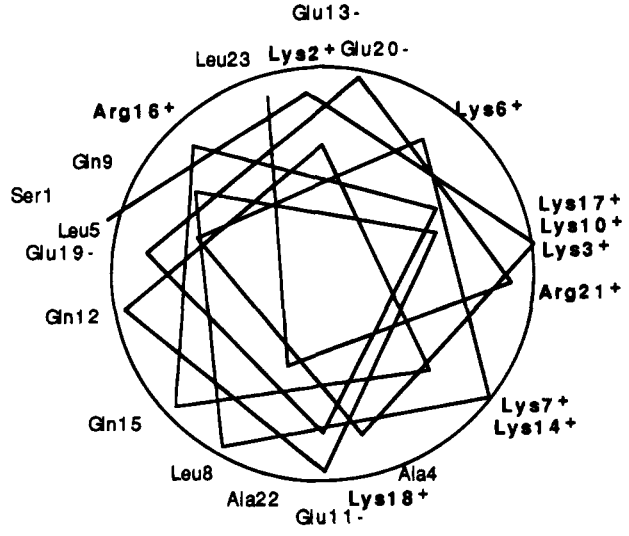

FIGURE 8: Projection of one of the tricosapeptide structures calculated along the helix axis displaying the location of the side-chain α-carbons along the peptide backbone. Eight cationic residues (boldface) are segregated to one face of the cylinder.

to a probable 1:1 stoichiometry for the interaction and a surprisingly high affinity constant.

Our result that one single conformation is to be seen from the NMR experiments with one single set of narrow resonances for every proton is to be paralleled with the situation encountered by Van der Graaf *et al.* (1992). These authors deduce possible mutually exchanging conformations for the bound peptide, resulting in the observed broadening of the resonances at the binding site. However, such a situation was not encountered by these authors for the binding to tetraphosphate. The present work should be paralleled also with the continuous efforts to design helical peptides capable of binding to charged substrates like heparin (Ferran *et al.*, 1992). The present study demonstrates that the propensity to significantly form α-helical structures on their own is probably not a prerequisite for the design of such active peptides. The interaction with a charged substrate having a spacing between the negative charges in the range of the distance between two residues separated by one helix turn (0.54 nm) would induce the helical structure. Ionic interactions would then be the dominant forces for the folding. It is probably of significance that a similar folding was found when the pH was raised to 11, leading to the neutralization of the lysine side chains, suppressing the unfavorable charge interactions.

Our results show that an asymmetrically charged peptide can interact with poly(phosphate)s and with poly(dT) or poly(dA), thus providing a structural motif that may participate in nonspecific nucleic acid−protein interactions. The putative involvement of this motif in the compartmentalization of lower eukaryotic aminoacyl-tRNA synthetases through dynamic electrostatic interactions with polyanionic components of the translation machinery (Ryazanov *et al.*, 1987; Mirande, 1991) raises the question whether the polyanion-induced α-helical transition of the synthetic peptide also occurs in the context of the intact protein. In this connection, it is noteworthy that yeast cytoplasmic native aspartyl-tRNA synthetase has failed to crystallize so far, whereas proteolytically modified enzyme deprived of its cationic NH_2-terminal extension could be readily crystallized (Lorber *et al.*, 1987). A plausible explanation is that interchain electrostatic repulsion between the cationic NH_2-terminal extensions of adjacent molecules hinders close packing of the dimeric enzyme into a crystalline lattice, a condition relieved by excision of these charges. On the other hand, the native enzyme could be crystallized in the presence of equimolar amounts of the cognate tRNA, but in this case, the first 65 residues from the NH_2-terminus were found to be disordered (Cavarelli *et al.*, 1993). This may suggest that enzyme-bound tRNA, by acting as a spacer between adjacent dimeric enzyme molecules, overcomes intermolecular charge repulsion due to the NH_2-terminal extensions, while persistence of unfavorable intramolecular charge interactions within the extensions favors a disordered structure. The results of the present study thus raise the possibility that the presence of equimolar amounts of octadecaphosphate may allow the crystallization of the native enzyme and may induce the α-helical transition of the relevant sequence at the NH_2-terminus, either in the absence or in the presence of equimolar amounts of the cognate tRNA.

ACKNOWLEDGMENT

We thank Professor Jeannine Yon and the Centre National de la Transfusion Sanguine (Les Ulis, Essonne, France) for access to the CD spectropolarimeter, Dr. Michel Desmadril for expert advice in CD measurements, and Professor André Tartar for his interest in this work.

REFERENCES

Billeter, M., Braun, W., & Wüthrich, K. (1982) *J. Mol. Biol. 155*, 321−346.

Brauchweiler, L., & Ernst, R. R. (1983) *J. Magn. Reson. 53*, 521−528.

Brünger, A. T. (1990) *X-Plor Manual*, Yale University, New Haven, CT.

Cavarelli, J., Rees, B., Ruffi, M., Thierry, J. C., & Moras, D. (1993) *Nature 362*, 181−184.

Cirakoglu, B., & Waller, J.-P. (1985) *Eur. J. Biochem. 149*, 353−361.

Crippen, G. M. (1977) *J. Comput. Phys. 24*, 96−107.

Davis, D. G., & Bax, A. (1985) *J. Am. Chem. Soc., 107*, 2821−2822.

Dobson, C. M., Olejniczak, E. T., Paulsen, F. M., & Ratcliffe, R. G. (1982) *J. Magn. Reson. 48*, 87−110.

Eriani, G., Dirheimer, G., & Gangloff, J. (1990) *Nucleic Acids. Res. 18*, 7109−7117.

Eriani, G., Prevost, G., Kern, D., Vincendon, P., Dirheimer, G., & Gangloff, J. (1991) *Eur . J. Biochem. 200*, 337−343.

Ferran, D. S., Sobel, M., & Harris, R. B. (1992) *Biochemistry 31*, 5010−5016.

Havel, T. F., Kuntz, I. D., & Crippen, G. M. (1983) *Bull. Math. Biol. 45*, 665−720.

Hennessy, J. P., & Johnson, W. C. (1982) *Anal. Biochem. 125*, 177−188.

Jeener, J., Meier, B. H., Bachmann, P., & Ernst, R. R. (1979) *J. Chem. Phys. 71*, 4546−4553.

Kline, A. D., Braun, W., & Wüthrich, K. (1988) *J. Mol. Biol. 204*, 675−724.

Kumar, A., Ernst, R. R., & Wüthrich, K. (1980) *Biochem. Biophys. Res. Commun. 95*, 1−5.

Kuntz, I. D., Crippen, G. M., & Kollman, P. A. (1979) *Biopolymers 18*, 939−957.

Lorber, B., Kern, D., Mejdoub, H., Boulanger, Y., Reinbolt, J., & Giege, R. (1987) *Eur. J. Biochem. 165*, 409−417.

Lorber, B., Mejdoub, H., Reinbolt, J., Boulanger, Y., & Giégé, R. (1988) *Eur. J. Biochem. 174*, 155−161.

Macura, S., & Ernst, R. R. (1980) *Mol. Physiol. 41*, 95−117.
Marion, D., & Wüthrich, K. (1983) *Biochem. Biophys. Res. Commun. 113*, 967−974.
Melki, R., Kerjan, P., Waller, J.-P., Carlier, M.-F., & Pantaloni, D. (1991) *Biochemistry 30*, 11536−11545.
Merrifield, R. B. (1963) *J. Am. Chem. Soc. 85*, 2149−2154.
Mirande, M. (1991) *Prog. Nucleic Acid Res. Mol. Biol. 40*, 95−142.
Mirande, M., & Waller, J. P. (1988) *J. Biol. Chem. 263*, 18443−18451.
Nilges, M., Clore, A., & Gronenborn, A. M. (1988) *FEBS Lett. 239*, 129−136.
Redfield, A. G., & Kuntz, S. D. (1975) *J. Magn. Reson. 19*, 250−254.
Ryazanov, A. G., Ovchinnikov, L. P., & Spirin, A. S. (1987) *Biosystems 20*, 275−288.
Sellami, M., Fasiolo, F., Dirheimer, G., Ebel, J.-P., & Gangloff, J. (1986) *Nucleic Acids Res. 14*, 1657−1666.
States, D. J., Haberkorn, R. A., & Ruben, D. J. (1982) *J. Magn. Reson. 48*, 286−292.
Stoven, V., Mikou, A., Piveteau, D., Guittet, E., & Lallemand, J. Y. (1989) *J. Magn. Reson. 82*, 163−168.
Strop, P., Wider, G., & Wüthrich, K. (1983) *J. Mol. Biol. 166*, 641−667.
Van der Graaf, M., Scheek, R. M., Van der Linden, C. C., & Hemmiga, M. A. (1992) *Biochemistry 31*, 9177−9182.
Wagner, R., & Wüthrich, K. (1979) *J. Magn. Resonon. 33*, 675−680.
Wishard, D. S., Sykes, B. D., & Richards, F. M. (1992) *Biochemistry 31*, 1647−1651.
Wüthrich, K., Wider, G., Wagner, G., & Braun, W. (1982) *J. Mol. Biol. 155*, 311−319
Wüthrich, K., Billeter, M., & Braun, W. (1983) *J. Mol. Biol. 169*, 949−961.
Wüthrich, K., Billeter, M., & Braun, W. (1984) *J. Mol. Biol. 180*, 715−740.
Yang, J. T., Wu, C. S., & Martinez, H. M. (1986) *Methods Enzymol. 130*, 208−269.
Zuiderweg, E. R. P., Kaptein, R., & Wüthrich, K. (1983) *Eur. J. Biochem. 137*, 279−292.